Available online at www.sciencedirect.com
ScienceDirect
Green Energy & Environment xxx (xxxx) xxx
www.keaipublishing.com/gee

Research paper

All-fluorinated electrolyte for non-flammable batteries with ultra-high specific capacity at 4.7 V

Zhe Wang [a,1], Zhuo Li [a,1], Jialong Fu [a], Sheng Zheng [a], Rui Yu [a], Xiaoyan Zhou [a], Guanjie He [b], Xin Guo [a,*]

[a] State Key Laboratory of Material Processing and Die & Mould Technology, Laboratory of Solid State Ionics, School of Materials Science and Engineering, Huazhong University of Science and Technology, Wuhan, 430074, PR China
[b] Electrochemical Innovation Lab, Department of Chemical Engineering, University College London, 20 Gordon Street, London WC1E 7JE, UK

Received 3 February 2023; revised 26 May 2023; accepted 11 June 2023
Available online ■ ■ ■

Abstract

Li metal batteries (LMBs) with $LiNi_{0.8}Mn_{0.1}Co_{0.1}O_2$ (NMC811) cathodes could release a specific energy of >500 Wh kg^{-1} by increasing the charge voltage. However, high-nickel cathodes working at high voltages accelerate degradations in bulk and at interfaces, thus significantly degrading the cycling lifespan and decreasing the specific capacity. Here, we rationally design an all-fluorinated electrolyte with addictive tri(2,2,2-trifluoroethyl) borate (TFEB), based on 3, 3, 3-fluoroethylmethylcarbonate (FEMC) and fluoroethylene carbonate (FEC), which enables stable cycling of high nickel cathode ($LiNi_{0.8}Co_{0.1}Mn_{0.1}O_2$, NMC811) under a cut-off voltage of 4.7 V in Li metal batteries. The electrolyte not only shows the fire-extinguishing properties, but also inhibits the transition metal dissolution, the gas production, side reactions on the cathode side. Therefore, the NMC811||Li cell demonstrates excellent performance by using limited Li and high-loading cathode, delivering a specific capacity >220 mA h g^{-1}, an average Coulombic efficiency >99.6% and capacity retention >99.7% over 100 cycles.

Keywords: Fluorinated electrolyte; Li metal batteries; Solid electrolyte interphase; Cathode electrolyte interphase; Coulombic efficiency

1. Introduction

The energy density of lithium-ion batteries (LIBs) has gradually approached the upper limit allowed by intercalation chemistry (300 Wh kg−1) [1–4]. One of the most advanced energy storage options to substantially promote the energy density towards 500 Wh kg^{-1} is regarded as LMBs with high-energy-density cathodes such as nickel-rich $LiNi_xMn_yCo_{1-x-y}O_2$ (NMC) and limited Li metal anodes [5].

On the cathode side, nickel-rich NMC cathodes provide a boosting energy density and power density by simply elevating the upper cut-off voltage [6]. However, this approach tends to induce structural degradation and parasitic reactions between electrolytes and highly reactive Ni^{4+}, which significantly degrades the cycling lifespan [7–9]. In addition, the hydrolysis of $LiPF_6$ in electrolytes produce HF acid under high cut-off voltages, further attacking NMC cathodes [11]. Such degradation become more serious in the case of $LiNi_{0.8}Mn_{0.1}Co_{0.1}O_2$ (NMC811) cathode at over 4.4 V cut-off voltages [4,10,11].

On the anode side, metallic Li has thermodynamic instability; continuous side reactions between electrolytes and Li anode decrease the cycling lifespan and the Columbic efficiency [1,12,13]. To keep high reversibility during cycling is critical when utilizing less lithium metal and less electrolyte

* Corresponding author. Distinguished Professor, School of Materials Science and Engineering, Huazhong University of Science and Technology, Wuhan, 430074, PR China. Tel./fax: +86 -27-8755-9804.
E-mail address: xguo@hust.edu.cn (X. Guo).
[1] Z. Wang and Z. Li contributed equally to this work.

https://doi.org/10.1016/j.gee.2023.06.002

[14]. Sustaining a satisfactory cycling lifespan is difficult under practical conditions, where high-loading cathodes, limited Li anodes and lean electrolyte are required to achieve high energy-density [12,15].

Degradations on the Li anode surface and the NMC811 cathode are normally caused by chemical groups in common commercial electrolytes. Designing a new electrolyte with desired compatibility with high loading NMC811 cathodes and Li metal anodes under >4.4 V voltages offer a promising solution for further development of LMBs with NMC811 cathodes. High-concentration electrolyte [16–20], localized high-concentration electrolytes [21–27] were invented to develop high-voltage batteries up to 4.4 V. However, high voltages reported in previous works are mostly below 4.7 V [14,31–33]. Up to now, most of these electrolytes are flammable, which is hazardous for safety operation of batteries [5,34]. All-fluorinated, non-flammable electrolytes have high ionic conductivity and a wide electrochemical stability window [28–30] Tri(2, 2, 2-trifluoroethyl) borate (TFEB) has a high oxidation potential and contains B atoms, so that it could be a potential co-solvent for all-fluorinated electrolytes [26]. Adding similar chemical Bifunctional nitrile-borate (TECB) into based electrolyte could improve the specific capacity to 158.7 mAh g^{-1} for the NMC811 cathode at a voltage of 4.7 V [27]. However, some research shows the electron-deficient B–O bonding character in TFEB may be a reason to cause the metal transition from NMC811 [26]. How to utilize TFEB to build up stable electrolytes for achieving higher specific capacity still is a field worth to be explored.

In this work, we designed and prepared a non-flammable, all-fluorinated electrolyte that contains 1.2 mol L^{-1} hexafluorophosphate ($LiPF_6$), with 20 vol.% co-solvent fluoroethylene carbonate (FEC), 60 vol.% major co-solvent 3, 3, 3-fluoroethylmethyl carbonate (FEMC), and 20 vol.% tri(2, 2, 2-trifluoroethyl) borate (TFEB). The electrolyte keeps good stability with 12 mg cm^{-2} (2.79 mAh cm^{-2}) high loading NMC811 and 50 μm lithium metal foil under 4.7 V. TFEB in combination with FEC solvents, plays a role of scavenger to remove H_2O and HF to prevent the decomposition of lithium hexafluorophosphate ($LiPF_6$). The all-fluorinated electrolyte achieves specific capacity over 220 mA h g^{-1}, and average Coulombic efficiency >99.7% after 100 cycles in NMC811||Li batteries working at 4.7 V.

2. Experimental section

2.1. Materials

Li metal foils (250 and 50 μm Li on Cu, 10 mAh cm^{-2}) were purchased from China Energy Lithium Co., Ltd. $LiNi_{0.8}Co_{0.1}Mn_{0.1}O_2$ cathodes were prepared according to Reference [14] (NMC811: conductive carbon: polyvinylidene fluoride (PVDF) = 9: 0.5: 0.5, by weight), where the areal loadings of active materials were about 12 mg cm^{-2} (2.79 mAh cm^{-2}) and 6 mg cm^{-2} (1.4 mAh cm^{-2}). Related details are shown in the supporting information.

2.2. Electrochemical measurements and characterizations

Electrolyte preparation and cell assembly/disassembly were conducted in an Ar-filled glove box with the moisture and O_2 contents below 0.1 ppm. The oxidative durability of different electrolytes was tested with Li||stainless steel (SS) cells. The processes of charging/discharging Li||Li Symmetric cells, Li||Cu cells, and NMC811||Li cells were determined using Land battery test stations (CT2001A, Wuhan Land Instruments). The current density for testing Li||Li Symmetric cells was 0.5 mA cm^{-2}. Li||Cu cells were tested at a current density of 0.5 mA cm^{-2}.

NMC811||Li cells were tested with voltages ranging from 3 to 4.7 V. Two cycles (1/10C, 20 mA g^{-1}) were pre-conducted for formation, afterwards, the formal long-term cycling test was started at a high charge/discharge current (1C). Moreover, long-term cycle-lifespan test of NMC811||Li full cells (N/P = 3.5) was conducted at a high charge/discharge current (0.3C) after the two formation cycles (1/10C, 20 mA g^{-1}). 50 μl electrolyte was added in coin cells. The glass fiber filters with different electrolytes were used to test the flammability.

2.3. Calculations

Theoretical calculations were conducted by means of the Density Functional Theory (DFT), details of which are given in the supporting information.

3. Results and discussion

Ni-rich layered cathodes normally face a series of detrimental processes in carbonate electrolytes. When working at a high-voltage, various organic species appear from carbonate solvents (CH_2−, C_2HO−, $ROCO_2Li$, Li_2CO_3, C–P and C–F) due to oxidation and decomposition, while $LiPF_6$ salt mainly decomposes into inorganic species (LiF, Li_3PO_4 and $Li_xPO_yF_z$), forming a thick CEI. Furthermore, $LiPF_6$ salt is prone to react with trace water to produce highly reactive POF_3, HF, HPO_2F_2 and HF. Seriously, HF in the electrolyte would not only attacks the cathode to damage the CEI, but also causes the leaching of transition metal ions from the cathode (as shown in Fig. 1(a) [35,36]. The transition metal ions will migrate to the anode to damage the anode SEI, hence resulting in capacity fading and dendrite growth. In contrast, the wide electrochemical stability window of all-fluorinated solvents with high ionic conductivity is promising to minimize Li depletion/pulverization and stabilize the NMC811 cathodes in LMBs (Fig. 1(b)).

The CF_3 of TFEB is a powerful electron-withdrawing chemical group which leads to a very low highest occupied molecular orbital (HOMO) energy value (Fig. 1(d)), enabling its extended oxidative stability [37–40]. Meanwhile, TFEB exhibits a lower lowest unoccupied molecular orbitals (LUMO) level compared with other typical solvents, and is thus preferentially reduced to form an SEI layer on Li anodes

Please cite this article as: Z. Wang et al., All-fluorinated electrolyte for non-flammable batteries with ultra-high specific capacity at 4.7 V, Green Energy & Environment, https://doi.org/10.1016/j.gee.2023.06.002

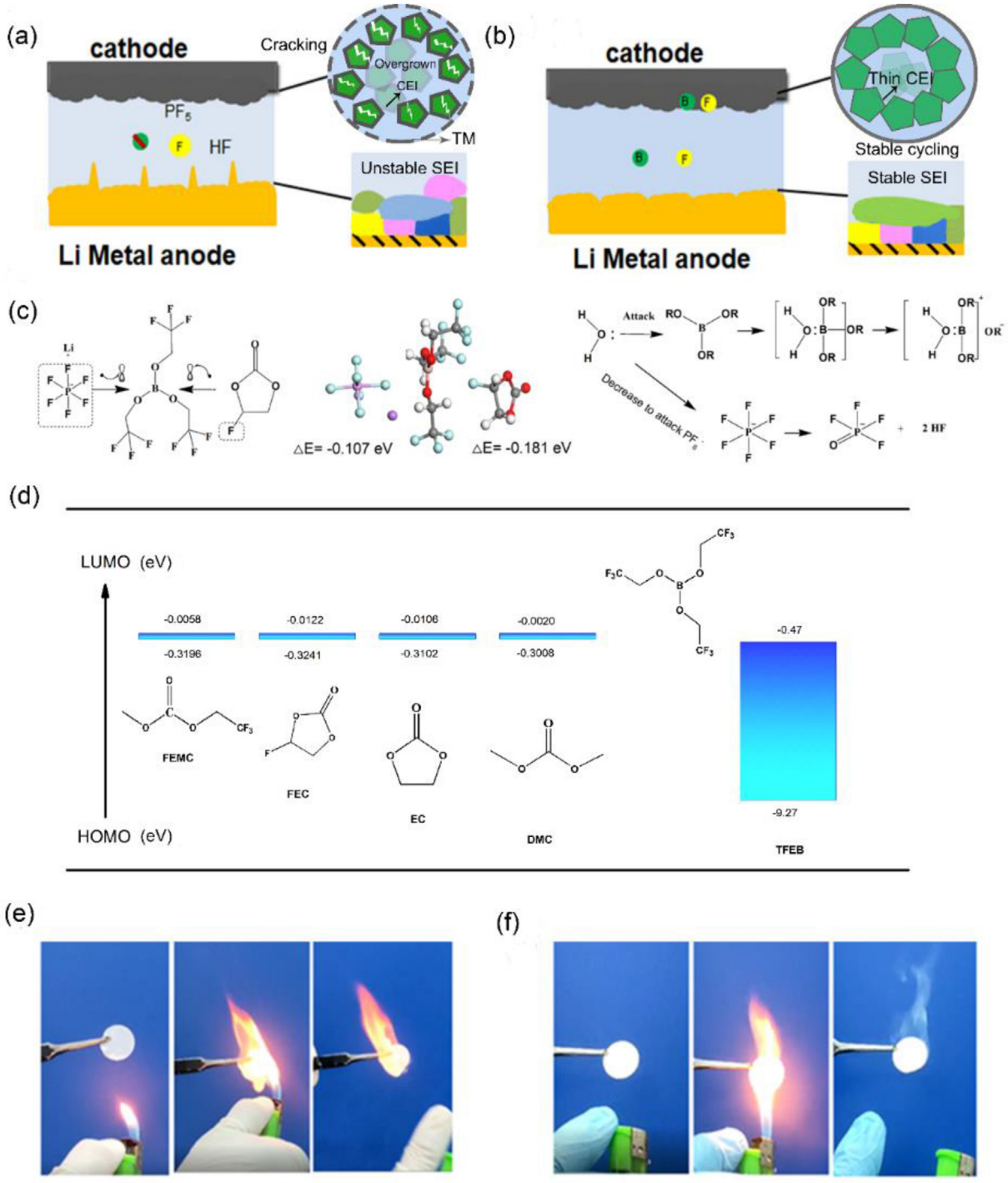

Fig. 1. Variation of SEI and CEI formed in different electrolytes: (a) traditional carbonate, and (b) fully fluorinated electrolyte. (c) Possible chemical combination mechanisms of TFEB with electron-rich chemical materials (FEC and $LiPF_6$) to form stable solvent structure and the pathway for removing trace H_2O by TFEB to decrease the $LiPF_6$ decomposition. (d) Comparison of the highest occupied molecular orbital (HOMO)-lowest unoccupied molecular orbital (LUMO) energy levels for commonly used Li salts and solvents including FEMC, FEC, EC, DMC, TFEB. (e) Flammability of traditional carbonate electrolyte, and (f) flame-retardant property of fully fluorinated electrolyte.

[37]. This priority is also confirmed by low reduction potential of TFEB, according to the calculated results in Fig. S2. Moreover, as demonstrated by the chemical electronic theory, the B atoms in TFEB can undergo a hydrolysis reaction due to an empty orbital in the sp^2 hybrid orbital [38], therefore, removing the trace water in the electrolyte (Fig. 1(c)) and decelerating $LiPF_6$ hydrolysis. Since TFEB is an electron-deficient boron compound, it is easy to be combined with electron-rich chemical materials, such $LiPF_6$, further reducing the decomposition of $LiPF_6$. The DFT calculation shows that

Please cite this article as: Z. Wang et al., All-fluorinated electrolyte for non-flammable batteries with ultra-high specific capacity at 4.7 V, Green Energy & Environment, https://doi.org/10.1016/j.gee.2023.06.002

the binding energy between TFEB and FEC is −0.181 eV and the binding energy between TFEB and $LiPF_6$ is −0.107 eV (Fig. 1(c)), proving that TFEB can combine with FEC and $LiPF_6$ to form stable solvated structure [38]. In addition, as a kind of fluorine-containing borate, TFEB is beneficial to the formation of thin B-contained CEI that is considered as good CEI component [12]. FEMC and FEC exhibit a lower HOMO than EMC and DMC, thus were selected as a co-solvent. Finally, the all-fluorinated electrolyte was prepared by dissolving 1.2 mol L^{-1} $LiPF_6$ salt into 60% volume FEMC, 20% volume FEC and 20% volume TFEB.

Concerning the safety operation, the commercial carbonate electrolyte ($LiPF_6$ in DMC/EC) and our all-fluorinated electrolyte ($LiPF_6$ FEC/FEMC/TFEB) were conducted for combustion experiments, as shown in Fig. 1(e and f). The $LiPF_6$/EC/DMC electrolyte is highly volatile and flammable, and it immediately caught fire and kept burning even after removing the fire. In sharp contrast, our all-fluorinated electrolyte did not burn.

The electrochemical stability of two electrolytes was investigated by LSV curves. As show in Fig. 2(a), the commercial carbonate-based electrolyte shows an oxidation potential of 4.4 V, while the all-fluorinated electrolyte shows an ultra-high voltage tolerance of >6 V, which is beneficial for promoting ultra-high voltage batteries. The cyclic voltammetry (CV) was used to test the oxidation/reduction stability of the commercial electrolyte, as shown in Fig. 2(b and c), CV curves show a large polarization in the commercial electrolyte. The all-fluorinated electrolyte exhibits a small reduction peak starting at 1.4 V (inserted graph in Fig. 2(b), enlarged view of CV curves), which corresponds to the SEI formation. The Li||Cu cell was assembled and tested for investigating the

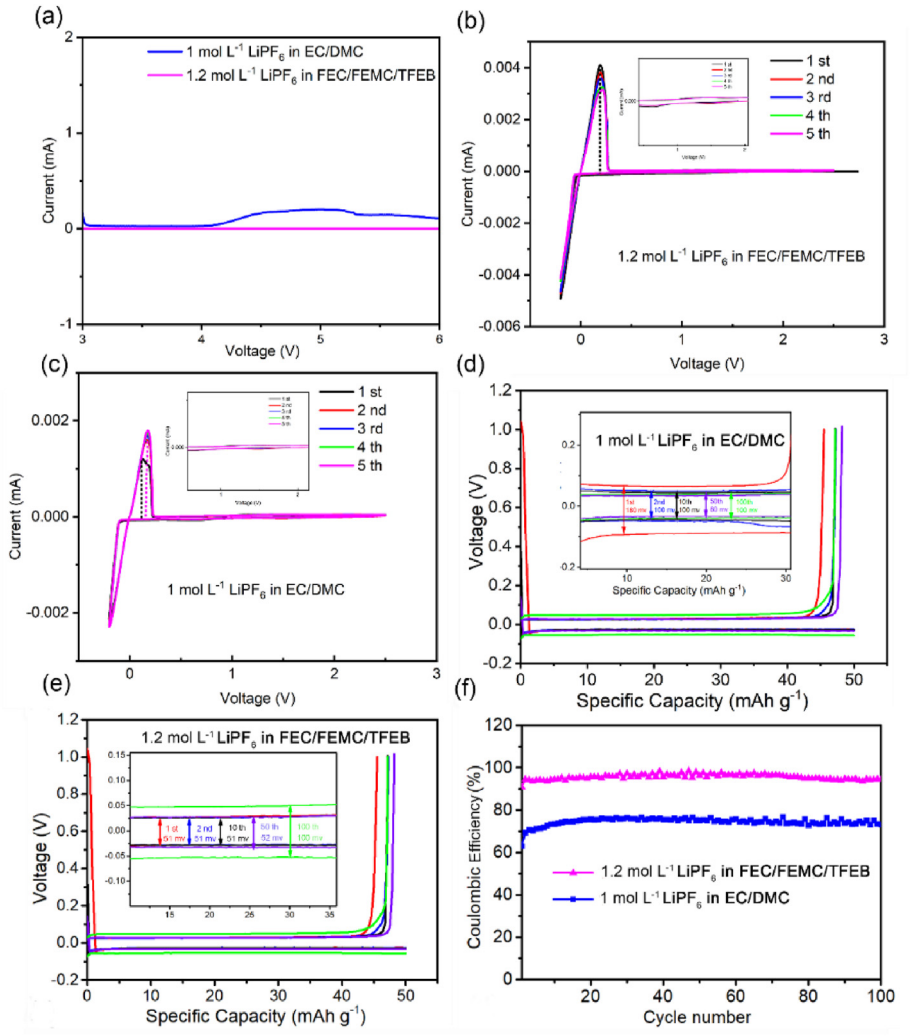

Fig. 2. (a) Oxidation stability of $LiPF_6$ FEC/FEMC/TFEB electrolyte and $LiPF_6$ EC/DMC electrolytes in Li||stainless steel cells measured by LSV at a scanning rate of 1 mV s^{-1}. (b) Oxidation/reduction stability of $LiPF_6$ EC/DMC electrolyte in Li||stainless steel cells measured by CV at a scanning rate of 2 mV s^{-1}. (c) Oxidation/reduction peak of $LiPF_6$ FEC/FEMC/TFEB fully-fluorinated electrolyte for forming SEI layer determined in Li||stainless steel cells and Oxidation/reduction stability of fully-fluorinated electrolyte by CV at a scanning rate of 2 mV s^{-1}. (d) Li-metal plating/stripping profiles on Cu foil cycled in $LiPF_6$ EC/DMC electrolyte at 0.5 mA cm^{-2}. (e, f) Li-metal plating/stripping profiles on Cu foil cycled in $LiPF_6$ FEC/FEMC/TFEB electrolyte at 0.5 mA cm^{-2}. Li plating/stripping Coulombic efficiency in different electrolytes at 0.5 mA cm^{-2}.

Please cite this article as: Z. Wang et al., All-fluorinated electrolyte for non-flammable batteries with ultra-high specific capacity at 4.7 V, Green Energy & Environment, https://doi.org/10.1016/j.gee.2023.06.002

cycling stability and Coulombic efficiency of Li metal anodes. As shown in Fig. 2(d–f), our all-fluorinated electrolyte can significantly increase the Li stripping/plating Coulombic efficiency (CE) and the cycling stability, and the Li plating/stripping Coulombic efficiency remains ~96% at 0.5 mA cm−2. In contrast, the reference electrolyte shows a Li Coulombic efficiency of 89.8%, much lower than that of the all-fluorinated electrolyte. Moreover, the all-fluorinated electrolyte shows a lower overpotential of ~52 mV, lower than that of the commercial $LiPF_6$/EC/DMC electrolyte (inserted graph in Fig. 2(d and e)).

Furthermore, our all-fluorinated electrolyte can also stabilize the NMC811 cathode. The NMC811||Li cell with the all-fluorinated electrolyte delivers an initial discharge-capacity of ~210 mA h g^{-1}, and retains 90.1% of its original capacity with an average Coulombic efficiency of 99.6% after 300 cycles at 1C (Fig. 3(a)). In contrast, the NMC811||Li cell with the commercial electrolyte shows a sudden drop both in Coulombic efficiency and capacity after 50 cycles, because of the over usage of active Li and the cathode degradations. Additionally, the NMC811||Li cell with the all-fluorinated electrolyte also exhibits excellent rate capability under ultra-high voltages, as shown in Fig. 3(d). Corresponding discharging capacities of the NMC811||Li cells at 1/10, 3/10, 5/10, 8/10, and 1C are 217.8, 208.5, 201.3, 194.6 and 191 mAh g^{-1}, respectively. After recovering the rate back to 0.1C, the capacity of 215 mAh g^{-1} can be achieved, remaining 98% of its initial capacity.

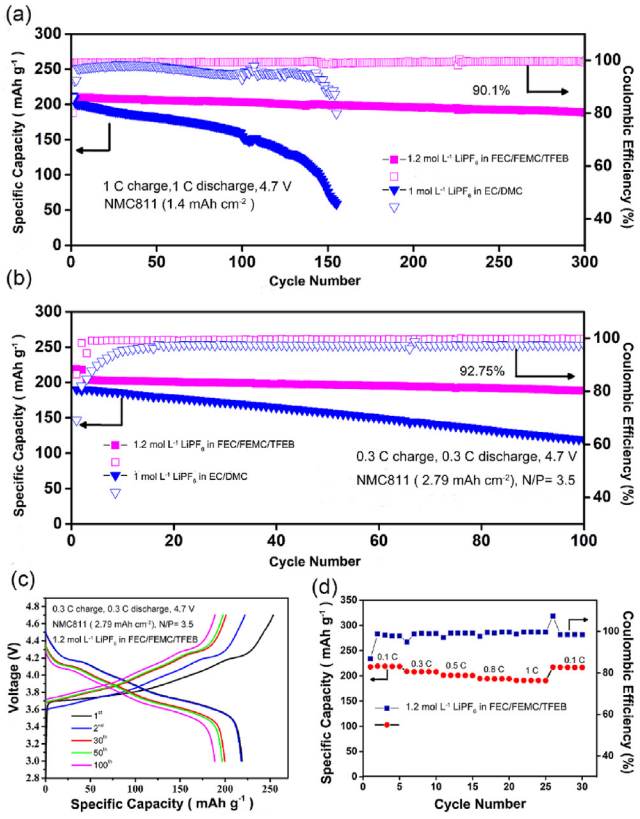

Fig. 3. Electrochemical performances of NMC811||Li cells: (a) Cycling performance of NMC811||Li cells with two different electrolytes at 1C. (b) Cycling performance of NMC811||Li full cells with two different electrolytes with N/P ≈ 3.5, under 0.3C charge and 0.3C discharge conditions, and (c) Corresponding voltage profiles of NMC811||Li full cell with $LiPF_6$ FEC/FEMC/TFEB at 0.3C (0.1C for the first and second cycles). (d) Corresponding rate performance of NMC811||Li cell with $LiPF_6$ FEC/FEMC/TFEB.

To maximize the energy density, the NMC811||Li full cell with a high-loading cathode (~2.6 mAh cm^{-2}), a 50 μm thick Li metal anode, and lean electrolyte (E/P = ~5 μL g^{-1}) were assembled and tested. When using the carbonate reference electrolyte, continuous decay exists in the NMC811||Li full cell under 4.7 V, showing an initial specific capacity of 195 mAh g^{-1}, capacity retention of 70% with an average CE of 95% after 100 cycles at 0.3C (Fig. 3(b and c)). However, under the same conditions, a significantly improved cycling performance was achieved using our all-fluorinated electrolyte in the NMC811||Li full cell, which achieves a capacity retention >92.75% after 100 cycles at 0.3C. Moreover, the electrolyte can release a higher specific capacity of 220 mAh g^{-1}; for comparison, related previous works are listed in Supplementary Table S3.

To better understand the stabilizing effect of our fluorinated electrolyte on the NCM811 cathode during charge/discharge process, CV curves of NMC811||Li metal batteries were measured and shown in Fig. S7. The experiment results show that all-fluorinated electrolyte has better stability, NMC811 with H1 phase transition could be observed by the peaks value change. The all-fluorinated electrolyte has less peak change, as compared with the commercial electrolyte, so that TM redox and phase transitions of NMC811 are suppressed in all-fluorinated electrolyte. Therefore, the experiment results demonstrate that our all-fluorinated electrolyte stabilizes the cathode better than the commercial electrolyte.

The Li pulverization problem was largely minimized in an NMC811||Li cell using the all-fluorinated electrolyte after long-term cycling. Fig. 4(a–f) show SEM images of the two Li metal anodes after 100 cycles. As shown in Fig. 4(a and b), the Li anode in the commercial electrolyte shows whisker-like Li deposits with highly porous, substantial cracking, and remarkable amount of “dead” Li. Moreover, active Li was completely consumed, causing the Li metal anode to swell hugely from 50 to ~200 μm in thickness (cross-view in Fig. 4(c)). Such an un-uniform Li deposition could cause impedance increase, cell failure and safety risk. Moreover, the above erosions would be worse and more dangerous with increasing cathode loading and charge voltage [41,42]. In contrast, for the cells using the all-fluorinated electrolyte, the Li particles remain large, uniform, and compact (Fig. 4(e and f)), and the thickness of less-compact layer is only ~48 μm (Fig. 4(f)).

To further characterize SEI compositions, X-ray photoelectron spectroscopy (XPS) was conducted for the Li anodes retrieved after 100 cycles. As shown in the C 1s spectra, C–C/C–H (~284.8 eV)/(~285.6 eV) are commonly observed species, and C–O (~285.7 eV), CO_3^{2-} (~289.3 eV) and poly (CO_3^{2-}) (~290.3 eV) [28] are presented in both electrolytes.

Please cite this article as: Z. Wang et al., All-fluorinated electrolyte for non-flammable batteries with ultra-high specific capacity at 4.7 V, Green Energy & Environment, https://doi.org/10.1016/j.gee.2023.06.002

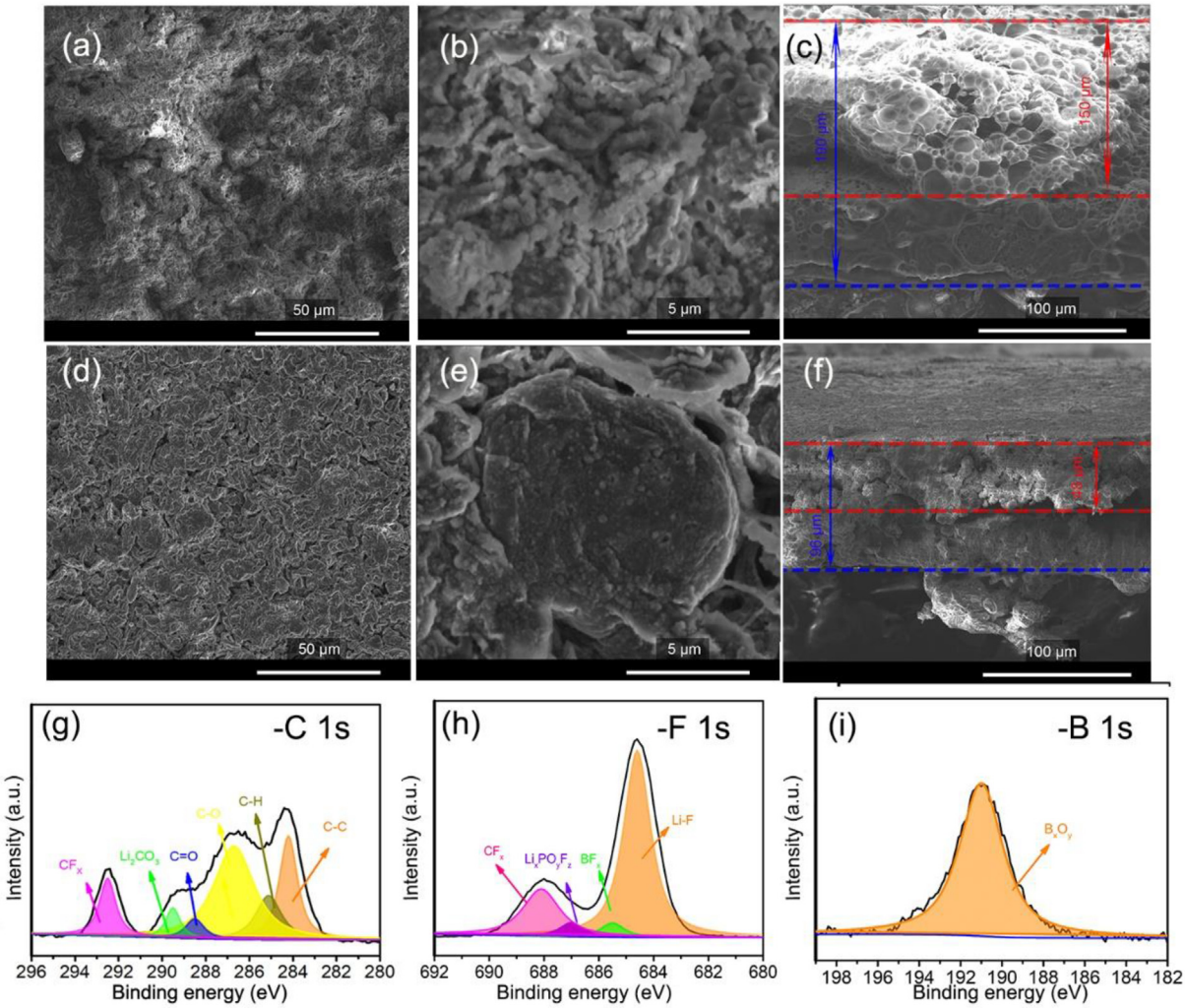

Fig. 4. SEM images of the 50 μm Li anode after 100 cycles in different electrolytes: (a–c) $LiPF_6$ EC/DMC, and (d–f) $LiPF_6$ FEC/FEMC/TFEB electrolytes. XPS spectra of the Li anode in $LiPF_6$ FEC/FEMC/TFEB after 100 cycles: (g) C 1s, (h) F 1s, (i) B 1s.

However, in the all-fluorinated electrolyte, some LiF (685 eV), $Li_xPO_yF_z$ (687 eV), B–F (685.5 eV) and CF_3 species can be found in the F 1s spectra. Notably, it shows a higher LiF (~685 eV) intensity and a less CFx (~688.5 eV) intensity in the all-fluorinated electrolyte than those in carbonate electrolytes. The existence of BxOy (~191 eV) is proved by the B 1s spectra [46], indicating that TFEB participates in the SEI formation. In the meantime, Li–B–O (~193 eV) and BF_2 (~195 eV) are rarely detected, which proves that the SEI may be filled with polymer-organic components derived from TFEB solvents. This kind SEI has better stability performance for resisting lithium dendrite growth [25,35].

The all-fluorinated electrolyte also facilitates the stable cycling of the NMC811 cathode under high voltages. The morphologies of the cycled NMC811 cathodes were characterized by SEM. As shown in Fig. 5(a), the NMC811 particles maintain spherical and smooth without obvious cracks. Different elements have been found on the CEI surface, including Ni, O, F, B, C and P elements (Fig. 5(b)). High content of F element and B element were detected on the NMC811 surface, confirming the formation of the F/B -rich interphase (Supplementary Table S2). HRTEM images (Fig. 5(c) and Fig. S3) display a thin and uniform CEI layer (~5 nm). Under the protection of the F/B-rich CEI, the degradation of Ni-rich cathodes can be suppressed [26].

To further characterize CEIs, XPS measurements were conducted on the surface of the cathode after 100 cycles, the results are shown in Fig. 5(d–f). Compared with the cathode cycled in the reference electrolyte (Fig. S4), the one cycled in our all-fluorinated electrolyte has a weaker C 1s signal (Fig. 4(g), the peaks can be attributed to C–C, C–H, CF_x, C–O, C=O, Li_2CO_3) and stronger F 1s (Li–F) and B 1s signals (B–F, Li–B–O), indicating that the CEIs derived from our electrolyte should consist of more B/F-like inorganic components (which are known to be 'good' CEI components [28]) and less organic components (decomposed from organic solvents). TFEB is much easier to combine with Li by B–O bonding because the reduction potential voltage is −6.913 V, while the positive reduction potential voltage of CF_3 and CH chemical groups is 1.261V and 1.581V, respectively (Fig. S2). In addition, BF_x

Please cite this article as: Z. Wang et al., All-fluorinated electrolyte for non-flammable batteries with ultra-high specific capacity at 4.7 V, Green Energy & Environment, https://doi.org/10.1016/j.gee.2023.06.002

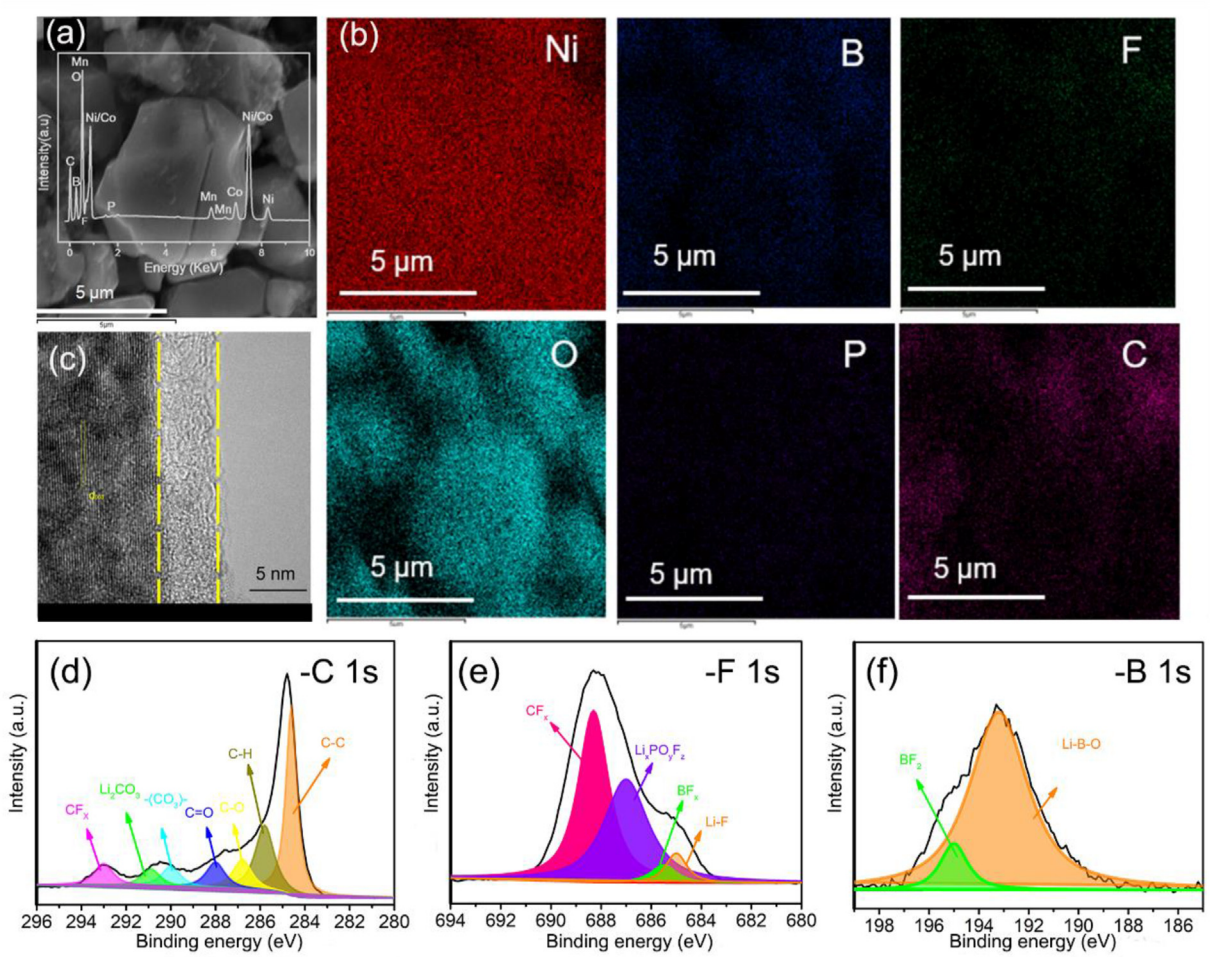

Fig. 5. Characterizations of cycled NMC811 cathodes in $LiPF_6$ FEC/FEMC/TFEB electrolyte: (a) SEM images of NMC811 cathode after 100 cycles in $LiPF_6$ FEC/FEMC/TFEB electrolyte, and the inset shows elements. (b) Elemental mappings of Ni, B, F, O, P, and C elements. (c) TEM image of the CEI layer on cycled NMC811. XPS spectra of NMC811 particles after 100 cycles: (d) C 1s, (e) F 1s, (f) B 1s.

could be a HF scavenger because B–F (613 kJ mol^{-1}) is more stable than H–F (565 kJ mol^{-1}) and P–F (490 kJ mol^{-1}) [47]. The XPS results also agree well with the elemental mapping, where more LiF_2 and $LiB_xO_yF_z$ components and fewer organic fragments were detected for the cathode cycled with our electrolyte.

F and B elements in our electrolyte help to form stable CEIs [49,50]. However, side reactions of the electrolyte on the NMC811 surface has potential risk to attack the CEI at high voltages. To further understand the oxidation behavior of electrolyte components under high voltages, PBE + U DFT calculations were conducted. Quantum chemistry calculations (Supplementary Table 2) predict that direct oxidation energies of all-fluorinated electrolyte components are all over 6.5 V. For the $LiPF_6$ − FEC based electrolyte, FEC•(−H) will attack SEI [50]. Calculated FEC oxidation potential stability value would drop to 3.10 V, if FEC•(−H) is oxidation products. Thus, co-solvent is very important to stabilize FEC•(−H), such as FEMC, HFE and DFEC [51]. FEMC and TFEB are stable co-solvents, because their oxidation potential stability values are all over 6 V in all conditions, as shown in Supplementary Table 2.

To explore major chemical components of CEI and side reactions on the NMC811 surface, reactions on the NMC811 surface are analyzed (Fig. 6). For FEC, reaction energy for the H transfer is negative (−1.57 eV), facilitating the production of FEC•(−H), while reaction energies of FEMC and TFEB are positive (4.26 eV and 4.28 eV, respectively), therefore, they are difficult to produce radicals. Compared with EC•(−H) radical, FEC•(−H) is a longer-lived radical [5]. Under high voltages, the oxidation side-products FEC•(−H) of positive electrodes may attack FEC carbonyl carbon to form aldehyde and alkyl carbonate oligomers, which causes the anode passivation [50]. In the meantime, TFEB has potential risk to cause the metal dissolution without other co-solvent. Moreover, as shown by the calculation result, the barrier for the radical ionization energy of FEC•(−H), FEMC•(−H) and TFEB•(−H) are all above 4.50 eV (Supplementary Table S2), indicating that the major chemical components of CEI come from the first step ionization. Therefore, there will probably be reactions among FEC•(−H), FEMC and TFEB to decrease side reactions and form fluorine-rich CEI. In addition, TFEB may react with FEC•(−H) to decrease the metal dissolution caused by TFEB on the cathode, while fluorinated groups could bond the

Please cite this article as: Z. Wang et al., All-fluorinated electrolyte for non-flammable batteries with ultra-high specific capacity at 4.7 V, Green Energy & Environment, https://doi.org/10.1016/j.gee.2023.06.002

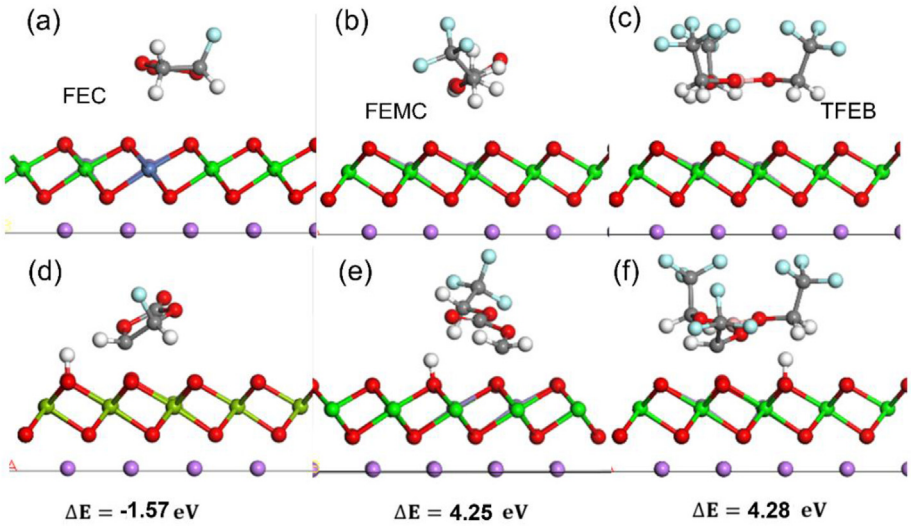

Fig. 6. Reaction activity of FEC, FEMC and TFEB solvents on fully charged NMC811 surface as calculated by PBE + U DFT. Reaction energies of initial (a–c) and final (d–f) configurations. $Ni_{0.8}Mn_{0.1}Co_{0.1}O_2$ surface shows NiO_6 octahedrons and CoO_6 octahedrons connected with MnO_4 octahedrons. ΔE, the energy difference between the physiosorbed solvent molecules and the reacted solvents. O, red; C, grey; F, light blue; H, white.

oxygen on NCM811 to prevent the OH formation and decrease metal dissolution.

4. Conclusions

We designed and prepared a fully fluorinated non-flammable electrolyte that can be applied for NMC811 cathodes under a high voltage of 4.7 V. After 200 cycles, our batteries achieved a high Coulombic efficiency of 99.7%, and an average specific capacity over 200 mA h g^{-1} at 1C. Remarkably, the NMC811||Li (N/P = 3.5) full cell with a high loading (12 mg cm^{-2}) cathode and thin lithium (50 μm) retained 92.75% of its original capacity after 100 cycles. The cycled Li anode and NMC811 cathode exhibited thin and smooth protective layers, which helped decreasing side reactions. Moreover, chemical analyses and DFT calculations revealed the mechanism to produce stable solvated structure based on TFEB and form highly stable CEI on the NMC811 surface. This work provides a new idea to apply TFEB on high voltage LMBs and lays a foundation for exploring more related electrolytes at over 4.7 V.

Declaration of competing interest

The authors declare that they have no known competing financial interests or personal relationships that could have appeared to influence the work reported in this paper.

Acknowledgements

All Authors would like to express their appreciation to the National Natural Science Foundation of China and the Israeli Science Foundation for funding this research within the framework of the joint NSFC-ISF grant # 51961145302. This work is also supported by China Postdoctoral Science Foundation funded project (Grant # 2020M682403).

Appendix A. Supplementary data

Supplementary data to this article can be found online at https://doi.org/10.1016/j.gee.2023.06.002.

References

[1] J.W. Choi, D. Aurbach, Nat. Rev. Mater. 1 (2016), 16013.
[2] J.B. Goodenough, Y. Kim, Chem. Mater. 22 (2009) 587–603.
[3] S.S. Zhang, ACS Appl. Energy Mater. 1 (2018) 910–920.
[4] D. Aurbach, E. Zinigrad, Y. Cohen, H. Teller, Solid State Ionics 148 (2002) 405–416.
[5] X. Fan, L. Chen, O. Borodin, X. Ji, J. Chen, S. Hou, T. Deng, J. Zheng, C. Yang, S.C. Liou, K. Amine, K. Xu, C. Wang, Nat. Nanotechnol. 13 (2018) 715–722.
[6] S. Ahmed, S.E. Trask, D.W. Dees, P.A. Nelson, W. Lu, A.R. Dunlop, B.J. Polzin, A.N. Jansen, J. Power Sources 403 (2018) 56–65.
[7] G. Ceder, Y.M. Chiang, D.R. Sadoway, M.K. Aydinol, Y.I. Jang, B. Huang, Nature 392 (1998) 694–696.
[8] A. Manthiram, J.C. Knight, S.T. Myung, S.M. Oh, Y.K. Sun, Adv. Energy Mater. 6 (2016), 1501010.
[9] J. Kim, H. Lee, H. Cha, M. Yoon, M. Park, J. Cho, Adv. Energy Mater. 8 (2018), 1702028.
[10] F. Ding, W. Xu, X.L. Chen, J. Zhang, M.H. Engelhard, Y.H. Zhang, B.R. Johnson, J.V. Crum, T.A. Blake, X.J. Liu, J.G. Zhang, J. Electrochem. Soc. 160 (2013) A1894–A1901.
[11] K. Xu, Chem. Rev. 114 (2014) 11503–11618.
[12] S. Li, Q. Liu, W. Zhang, L. Fan, X. Wang, X. Wang, Z. Shen, X. Zang, Y. Zhao, F. Ma, Y. Lu, Adv. Sci. 8 (2021), 2003240.
[13] Y.K. Sun, S.T. Myung, B.C. Park, J. Prakash, I. Belharouak, K. Amine, Nat. Rev. Mater. 8 (2009) 320–324.
[14] X.D. Ren, L.F. Zou, X. Cao, M.H. Engelhard, W. Liu, S.D. Burton, H.K. Lee, C.J. Niu, B.E. Matthews, Z.H. Zhu, C.M. Wang, B.W. Arey, J. Xiao, J. Liu, J.G. Zhang, W. Xu, Joule 3 (2019) 1662–1676.
[15] W.J. Xue, M.J. Huang, Y.T. Li, Y.G. Zhu, R. Gao, X.H. Xiao, W.X. Zhang, S.P. Li, G.Y. Xu, Y. Yu, P. Li, J. Lopez, D.W. Yu, Y.H. Dong, W.W. Fan, Z. Shi, R. Xiong, C.J. Sun, I. Hwang, W.K. Lee, Y. Shao-Horn, J.A. Johnson, J. Li, Nat. Energy 6 (2021) 495–505.
[16] X. Cao, H. Jia, W. Xu, J.G. Zhang, J. Electrochem. Soc. 168 (2021), 010522.

[17] J. Zheng, J.A. Lochala, A. Kwok, Z.D. Deng, J. Xiao, Adv. Sci. 4 (2017), 1700032.
[18] Y. Yamada, A. Yamada, J. Electrochem. Soc. 162 (2015) A2406–A2423.
[19] L. Suo, D. Oh, Y. Lin, Z. Zhuo, O. Borodin, T. Gao, F. Wang, A. Kushima, Z. Wang, H.C. Kim, Y. Qi, W. Yang, F. Pan, J. Li, K. Xu, C. Wang, J. Am. Chem. Soc. 139 (2017) 18670–18680.
[20] J. Qian, W.A. Henderson, W. Xu, P. Bhattacharya, M. Engelhard, O. Borodin, J.G. Zhang, Nat. Commun. 6 (2015) 6362.
[21] N. Piao, X. Ji, H. Xu, X.L. Fan, L. Chen, S.F. Liu, M.N. Garaga, S.G. Greenbaum, L. Wang, C.S. Wang, X.M. He, Adv. Energy Mater. 10 (2020), 1903568.
[22] J. Zheng, X.L. Fan, G.B. Ji, H.Y. Wang, S. Hou, K.C. DeMellac, S.R. Raghavana, J. Wang, K. Xue, C.S. Wang, Nano Energy 50 (2018) 431–440.
[23] L. Suo, Y.-S. Hu, H. Li, M. Armand, L. Chen, Nat. Commun. 4 (2013) 1481.
[24] X. Fan, L. Chen, X. Ji, T. Deng, S. Hou, J. Chen, J. Zheng, F. Wang, J. Jiang, K. Xu, C. Wang, Chem 4 (2018) 174.
[25] F. Huang, G. Ma, Z. Wen, J. Jin, S. Xu, J. Zhang, J. Mater. Chem. A. 6 (2018) 1612.
[26] X. Cao, P. Gao, X. Ren, L. Zou, J.G. Zhang, Proc. Natl. Acad. Sci. USA 118 (2021), e2020357118.
[27] F. Liu, Z. Zhang, Z. Yu, X. Fan, M. Yi, M. Bai, Y. Song, Q. Mao, B. Hong, Z. Zhang, Chem. Eng. J. 434 (2022), 134745.
[28] T. Deng, X.L. Fang, L.S. Cao, J. Chen, S.Y. Hou, X. Ji, L. Chen, S. Li, X.Q. Zhou, E.Y. Hu, D. Su, X.Q. Yang, C.S. Wang, Joule 3 (10) (2019) 2550–2564.
[29] Q. Zheng, Y. Yuki, S. Rui, K. Seongjae, Y.Y. Lee, K. Kim, E. Nakamura, A. Yamada, Nat. Energy 5 (2020) 291–298.
[30] L. Suo, W. Xue, M. Gobet, S.G. Greenbaum, C. Wang, Y. Chen, W. Yang, Y. Li, J. Li, Proc. Natl. Acad. Sci. U.S.A. 115 (2018) 1156–1161.
[31] L. Yu, S.R. Chen, H. Lee, L.C. Zhang, M.H. Engelhard, Q.Y. Li, S.H. Jiao, J. Liu, W. Xu, J.G. Zhang, ACS Energy Lett. 3 (2018) 2059–2067.
[32] J.M. Zheng, S.R. Chen, W.G. Zhao, J.H. Song, M.H. Engelhard, J.G. Zhang, ACS Energy Lett. 3 (2018) 315–321.
[33] X.D. Ren, S.R. Chen, H. Lee, D.H. Mei, M.H. Engelhard, S.D. Burton, W.G. Zhao, J.M. Zheng, Q.Y. Li, M.S. Ding, M. Schroeder, J. Alvarado, K. Xu, Y.S. Meng, J. Liu, J.G. Zhang, W. Xu, Chem 4 (2018) 1877–1892.
[34] Z. Li, H.M. Huang, J.K. Zhu, J.F. Wu, H. Yang, L. Wei, X. Guo, ACS Appl. Mater. Interfaces 11 (2019) 784–791.
[35] Q.F. Zheng, Y. Yamada, R. Shang, S. Ko, Y.Y. Lee, K. Kim, E. Nakamura, A. Yamada, Nat. Energy 5 (2020) 291–298.
[36] Y.B. Liu, L. Tan, L. Li, J. Power Sources 221 (2013) 90–96.
[37] X. Cao, X.D. Ren, L.F. Zou, M.H. Engelhard, W. Huang, H.S. Wang, B.E. Matthews, H. Lee, C.J. Niu, B.W. Arey, Y. Cui, C.M. Wang, J. Xiao, J. Liu, W. Xu, J.G. Zhang, Nat. Energy 4 (2019) 796–805.
[38] X.X. Zuo, C.J. Fan, J.S. Liu, X. X, J.H. Wu, J.M. Nan, J. Power Sources 229 (2013) 308–312.
[39] Y. Zheng, F.A. Soto, V. Ponce, J.M. Seminario, X. Cao, J.G. Zhang, P.B. Balbuena, J. Mater. Chem. A 7 (2019) 25047–25055.
[40] X. Cao, P.Y. Gao, X.D. Ren, L.F. Zou, M.H. Engelhard, B.E. Matthews, J.T. Hu, C.J. Niu, D.Y. Liu, B.W. Arey, C.M. Wang, J. Xiao, J. Liu, W. Xu, J.G. Zhang, P. Natl. Acad, Sci. USA 118 (2021), e2020357118.
[41] T. Zheng, J. Xiong, X. Shi, B.Y. Zhu, Y.J. Chen, H.B. Zhao, Y.G. Xia, Energy Storage Mater. 38 (2021) 599–608.
[42] P. Bai, J. Li, F.R. Brushetta, M.Z. Bazant, Energy Environ. Sci. 10 (2016) 3221–3229.
[46] F. Cheng, X. Zhang, Y. Qiu, J. Zhang, Y. Huang, Nano Energy 88 (2021), 106301.
[47] Y.X. Li, W.K. Li, R. Shimizu, D.V. Cheng, H.N. Nguyen, J. Paulsen, S. Kumakura, M.H. Zhang, Y.S. Meng, Adv. Energy Mater. 12 (2022), 2103033.
[49] J. Zhang, H. Wu, X. Du, H. Zhang, L. Huang, F. Sun, T. Liu, S. Tian, L. Zhou, S. Hu, Z. Yuan, B. Zhang, J. Zhang, G. Cui, Adv. Energy Mater. 13 (2023), 2202529.
[50] D. Aurbach, E. Markevich, G. Salitra, J. Am. Chem. Soc. 143 (2021) 21161–21176.
[51] T. Li, X.Q. Zhang, P. Shi, Q. Zhang, Joule 3 (2019) 2647–2661.

Please cite this article as: Z. Wang et al., All-fluorinated electrolyte for non-flammable batteries with ultra-high specific capacity at 4.7 V, Green Energy & Environment, https://doi.org/10.1016/j.gee.2023.06.002